(Preprint) AAS ID-563

RELATIVE DYNAMIC MODEL SELECTION TO MAXIMISE EVASIVE MANOEUVRES EFFECTIVENESS

Filippo Mascellani*, Laura Oliva†, Michele Maestrini‡, Luigi De Maria§

This work investigates the influence of relative dynamics model selection on the effectiveness of real-time evasive strategies in orbital Pursuit-Evasion games under angles-only navigation. In scenarios where spacecraft rely solely on passive optical measurements and low-thrust control, the observability, fidelity, and computational load of the selected model critically impact the manoeuvrer outcome. Several linear and nonlinear models are evaluated within a State-Dependent Riccati Equation control framework. After establishing observability via Lie derivative analysis, a comprehensive sensitivity study assesses each model's performance across varying orbital regimes and relative initial conditions. Results reveal significant variations in control efficiency and game duration depending on the dynamics used, even under full-information assumptions. The Xu-Wang model offers the best balance of accuracy and feasibility, while lighter models like Tschauner-Hempel remain suitable for constrained systems. The findings support adaptive and dynamic model selection for robust autonomous defence.

INTRODUCTION

Space has become a critically contested and strategic frontier, due to the increasing amount and significance of the data and services derived from space assets, essential for both civil and military functions. However, this reliance introduces increasing vulnerabilities that may expose and disrupt space operations, causing widespread outages.

Today, those threats can be mainly categorised into two families: kinetic and cybernetics attacks. The former considers all hostile interactions involving malicious interceptions aimed at crashing or damaging the target or non-cooperative rendezvous, whilst the latter less dramatic tactic, considers jamming and spoofing at a safe distance.

Moreover, the situation is worsened by the indirect disruptions that may arise from such attacks, such as a derelict spacecraft losing control functions and colliding with another.

In this framework, autonomous and resource-efficient defensive tactics become critical to mitigate such risks through real-time evasive manoeuvres. Furthermore, those technologies should comply with the current autonomy and miniaturisation trends, focused on computational burden, mass, volume and power requests, to provide a meaningful solution to the increasing tensions arising in space.

In the miniaturisation framework embraced by the space industry, Angles Only Navigation (AON) has gained significant traction. This is because this technique estimates the relative position, and possibly attitude, of a target through angular measurements only, also referred to as Line-Of-Sight (LOS) versor, obtained from passive and compact cameras, without the need for active, voluminous and high power-consuming sensors like radar or lidars.

However, this measurement set introduces some complications, as the accuracy and reliability of the state estimations are affected, particularly as the inter-spacecraft separation increases due to the behaviour of angular measurement, but also the system observability is negatively influenced. This means that the defending asset

*PhD Candidate, Department of Aerospace Science and Technology, Politecnico di Milano, Milano, Italy.
†Space Engineer, Department of Aerospace Science and Technology, Politecnico di Milano, Milano, Italy.
‡Assistant Professor, Department of Aerospace Science and Technology, Politecnico di Milano, Milan, Italy.
§PhD Candidate, Department of Aerospace Science and Technology, Politecnico di Milano, Milan, Italy.

estimation capabilities may be highly hindered in realistic defensive scenarios where the players do not share common knowledge.[1,2]

On the other hand, the work by Gong[3] presents four solutions to mitigate those issues arising, particularly gaining full state observability with AON. The first solution is to complicate the dynamic modelling, then comes multi-LOS configurations, sensors offsets and orbital manoeuvres. However, of all methods provided, multi-LOS does not fit the scenario at hand, as a single object is considered, and the same stands for sensors offset, as it is reasonable to assume the escaping object to have physical sizes that prevent a meaningful baseline separation across measurements, particularly as the distances increase, thus allowing for increased observability when the attacker is already too close to the evader to escape. A similar point stands for the orbital manoeuvres, as the pursuer may actively manoeuvre to limit its detectability, beyond gaining an advantage within the game. Hence, the preferred solution is to introduce more complex dynamic models.

The mathematical formulation of such techniques can be framed and formalised to space objects through the Pursuit Evasion (PE) game theory, a concept first introduced in 1965.[4]

In its simplest form, a two-player game is investigated, with one player, the evader, aiming to escape the threats of the malicious attacker, the pursuer. The dynamics of these games are governed by continuous decision-making processes, where each player shall evaluate the anticipated actions of the opponent based on some case-specific cost function, referred to as the value of the game, beyond the system dynamics itself, described by differential equations. Additionally, Isaacs[4] also proposes a hierarchy of games, distinguishing between Zero-Sum Games (ZSG), where the game's objectives of each player are equal to each other, and Non-Zero Sum Games (NZSG), introducing different goals along the game for each player. This hierarchy can be further complicated by introducing the information game,[5] with the concepts of imperfect and uncertain games, where the concurrent actions of state uncertainty arising from sensors' noise and imperfect modelling, respectively, trigger inaccuracies in the system dynamics.

Existing state-of-the-art PE game solutions present some intricacies as they either rely on highly detailed and complex dynamics that exploit impractical solving strategies for on-board implementation,[6,7] or they use oversimplified dynamic approaches that compromise the real-world fidelity and applicability of the solution,[1,8,9] such limiting the modelling of perturbations, or the system observability when optical measurements are deployed.[1]

Examples of the first case are the foundational work from Pontani,[10] investigating the numerical solution of the optimal manoeuvres problem through a Genetic Algorithm (GA) alongside a semi-direct collocation nonlinear programming, bypassing the solution of a Two-Point Boundary Value Problem (TPBVP), yet also assuming constant acceleration, leading to suboptimal strategies.

Stupik[11] provides a similar method exploiting the Hill-Clohessy-Wiltshire (HCW) equations and a particle swarm optimisation to solve a reduced TPBVP.

The flaws of this method are tackled by Shen and Casalino,[6] accounting for varying thrust-to-mass ratio, advancing the indirect shooting method by incorporating one-sided optimisation outcomes. Also Li et al. address the variable mass issue by proposing the combined shooting and collocation method to solve PE games. By employing analytical conditions and decomposing the TPBVP into two layers, the method can robustly compute accurate saddle-point strategies in various scenarios, with a diminished computational burden.

In similar works that provide solutions that are too demanding for miniaturised onboard computations, Horie and Conway[12] exploit a semidirect collocation nonlinear programming, merging a GA and one-sided optimisation problem.

On the other hand, as mentioned above, other studies rather focus on the feasibility of the implementation. Here, one finds the work by Jagat and Sinclair,[8] framing the PE game as a fixed time linear quadratic regulator, assuming complete information, and the derived control law is extended to nonlinear models through the State Dependent Riccati Equation (SDRE).

Blasch et al.[13] focus on PE game in a sensor management context and propose various onboard filtering strategies for target tracking, solving the problem in a MATLAB environment.

Other works, instead, cannot be strictly categorised as they employ both simplified dynamic models and computationally intensive strategies. Examples are the work from Sun et al. introducing a hybrid semi-direct control parametrisation and multiple shooting, based on HCW dynamics. However, this estimation-based escape strategy is shown to be robust against changing values of the objectives during the game, a result that

no other work was able to provide.
This research examines the impact of different relative dynamic models on the PE game evolution in an SDRE framework. It wants to emphasise the feasibility for onboard implementation and the robustness over a wide range of orbital scenarios, showing that, even though both players know exactly each other's state and objective, varying the dynamic modelling leads to non-negligible variations in defensive strategies. Additionally, a player might gain an advantage over the other through a more accurate and complete model in the SDRE control computation.
Rooted in the design and development of an entirely autonomous and real-time evasive pipeline aiming to defend against attacking objects whose initial relative state and objectives are unknown and uncertain state and need to be estimated through AON, this work shows the first step considered: selecting a dynamic model that allows for system observability, and accurate estimations, whilst providing high fidelity propagation and controls throughout the engagement. In order to provide a comprehensive and clear analysis starting from the problem foundations to then move to the consequences of various design choices, the remainder of the work is structured as follows: Section 2 reports the theoretical concepts behind the work, including the reference frames, controls and PE game formulations, ending with the presentation of the dynamic models selected for the analysis.
Section 3 presents the dynamics sensitivity analyses executed on the inertial and relative game conditions for the various scenarios. Section 4 presents the consequences and analysis of the introduction of the preferred dynamic in the PE game, assessing how different dynamic models react to variations in reciprocally known variables, showcasing their dependencies.
Section 5 presents conclusions and future works.

FUNDAMENTALS

This section reports the theoretical foundation underlying the methodologies explored in the work to establish a clear baseline.

Reference Frames

To rigorously express the position and velocity components of the objects considered, a precise definition of the reference frames exploited is strictly mandatory. This work employs two primary reference frames: the Earth-Centred Inertial (ECI) frame, which locates objects in their motion around Earth, and the Local Vertical Local Horizontal (LVLH) frame, commonly deployed to characterise the relative motion of objects in space with respect to the central body. These frames provide the geometric and dynamic foundation for orbital propagation and relative motion modelling.[14]
The frames are reported superimposed one onto the other in Figure 1.
The ECI reference frame, denoted as $I = \{X, Y, Z\}$, is a quasi-inertial coordinate system with origin at the Earth's centre of mass, the Z axis aligned with the mean rotation axis, or celestial north, the X axis pointing towards the mean vernal equinox of epoch J2000, and the Y axis complete the orthogonal right-handed triad.
The LVLH frame, denoted as $L = \{ x, y, z \}$, is a body-fixed, rotating frame centred on the target spacecraft barycentre or to a virtual reference point on a nominal orbit.[14] This frame considers the x-axis pointing radially outward from Earth to the spacecraft, the z-axis aligned to the positive angular momentum vector, and y completes the right-handed triad, pointing in the along-track direction.

Dynamic Model Selection

In the vast framework of spacecraft relative motion modelling, the available dynamic models are highly diverse in terms provided accuracy and stability, of the deployed modelling variables, their number and physical meaning as well as subject to a multitude of constraints and limitations to maintain accurate propagation, in terms of allowed inter-spacecraft separation, particularly for linearised models, eccentricity of the orbit, the modelled perturbations and their variable modelling accuracy. Lastly, the computational burden links all those elements together.
Following an in-depth analysis of the existing literature reviews of relative motion models,[15–18] the most

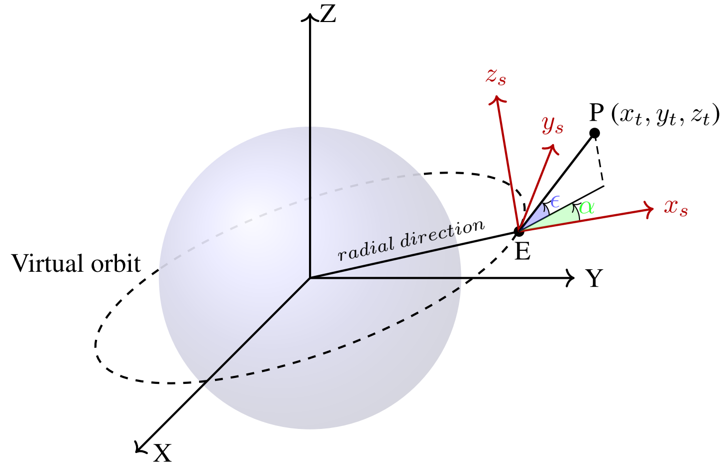

Figure 1: ECI and LVLH reference frames[14]

promising dynamic models for flexible on-board implementations are selected and illustrated in Figure 2, with their characteristics explicated below.

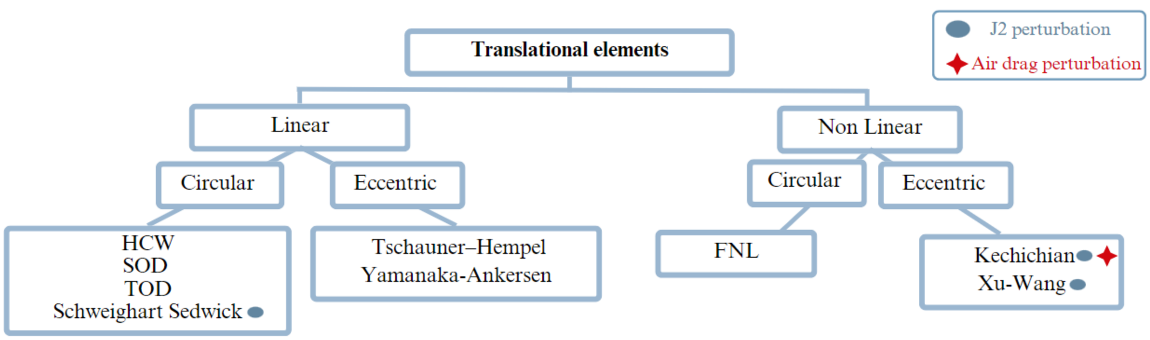

Figure 2: Translational elements classification

Notably, to provide a robust foundation, the research focuses on the rather established Cartesian elements representation, exploiting the position vector $\rho = [x\ y\ z]$ and velocity $\dot{\rho} = [\dot{x}\ \dot{y}\ \dot{z}]$ of an object in a defined reference frame, so that a six-dimensional relative state is defined as $\mathbf{x} = [\rho \ddot{\rho}]$, both in the ECI and LVLH frames.

First, the canonical HCW[19] equations provide an efficient linearised solution for circular orbits. However, its non-observability with AON, regardless of the number of measurements and sensors, forces its exclusion a priori as the estimation of unknown quantities proves unfeasible.[20] In the same work, solutions are proposed to the non-observability by expanding the HCW equations to higher orders expansions: Second Order Dynamics (SOD), Third Order Dynamics (TOD) and Full Non-Linear (FNL).

Sedwig and Schweighart expand those[21] (SCSW) by incorporating the J_2 perturbation, yet requiring the solution of an implicit equation at each time step, impacting the autonomy robustness, presenting an increased trade-off between accuracy and computational cost.

While the methods just mentioned apply to circular orbits, Tschauner and Hempel[22] (TH) provide a solution for elliptical orbits, with Yamanaka and Ankersen[23] (YA) proposing a closed-form solution to the TH equation, devising a state transition matrix that optimises the computational burden.

On the other hand, other highly non-linear approaches are designed to meet the suggestions by Gong,[3] including perturbations. Those include the Kechichian model (KE),[24] comprising air drag and Earth oblateness, and the Lagrangian mechanics-based Xu-Wang[25] (XW) model, with Earth oblateness only. Those models, in principle, should enhance the system observability and propagation accuracy, although weighing on computations. One should also notice that the latter two methods comprise twelve variables, despite the canonical six of the other models, as the inertial motion of the spacecraft around which the relative motion is also modelled.

Control Theory

Differential games can be formulated as problems in which two players attempt to achieve their opposite objectives optimally.
In the theory of optimal control, the linear quadratic regulator (LQR) represents the fallback solution when the aim is to minimise the costs of controlling a system's dynamics, expressed as differential equations, with respect to a reference desired condition. However, due to the AON observability issues, this formulation needs to be adapted to handle non-linear, more complex systems, whilst enabling more realistic control computation. This is solved through the SDRE formulation. This method considers the factorisation, that is, parameterisation, of the non-linear system dynamics into the product of the state vector and a matrix-valued function that depends on the state itself, through State-Dependent Coefficients (SDC) matrices, leading to a non-unique linear structure, minimising the nonlinear performance index through a quadratic-like structure, despite the non-unique representation preventing the solution's optimality.
By framing the PE game in an infinite time horizon problem, the LQR cost function's final term is neglected, solving an Algebraic Riccati Equation (ARE) through the SDC matrices at each game time instance. Notably, the non-unique parametrisation allows for an extra degree of freedom, enhancing the controller's optimality based on the scenario.
The SDRE cost function for time-infinite horizons is reported in Equation 1. The minimisation or maximisation of this cost function index leads to the two players minimising and maximising relative distance and velocity, depending on their objective: impact or evasion.

$$J = \frac{1}{2}\int_{t_0}^{\infty}(\boldsymbol{x}(t)^T Q\boldsymbol{x}(t) + \boldsymbol{u}(t)^T R\boldsymbol{u}(t))dt \tag{1}$$

Then the near-optimal controls are computed through the symmetric matrix P, the solution of the ARE reported in Equation 2:

$$0 = A^T(\boldsymbol{x})P(\boldsymbol{x}) + P(\boldsymbol{x})A(\boldsymbol{x}) + Q(\boldsymbol{x}) - P(\boldsymbol{x})(B(\boldsymbol{x})R(\boldsymbol{x})^{-1}B(\boldsymbol{x}))P(\boldsymbol{x}) \tag{2}$$

So the control action is:

$$\boldsymbol{u}(t) = -R(\boldsymbol{x})^{-1}B(\boldsymbol{x})^T P(\boldsymbol{x})\boldsymbol{x} \tag{3}$$

In the cost function of Equation 1, the Q matrix penalises deviations from the desired state, hence, a higher value leads to enhanced control actions. On the other hand, R penalises the control efforts in the cost function so that a large value of R introduces a higher penalty for the same control actions, favouring lower and less aggressive controls. This formulation of the PE game, finds the suboptimal controls for each player corresponding to a saddle point solution, or Nash equilibrium.[26] This solution is such that any player deviating from it unilaterally will worsen their situation, as a result of the payoff variation opposite to the player's objective, granting an advantage to the opponent.

METHODOLOGIES

In this section, the analyses carried out are explained, together with the techniques and design decisions required.

Dynamic Models Performance Analysis

The previously selected relative dynamic model's performance is analysed from multiple perspectives, aiming to identify the model that best meets the user demands, individuated as: the computational efficiency,

measured through computing time, the global propagation accuracy, expressed by the Root Mean Square Error (RMSE) of each relative state component, and the local accuracy, represented by the maximum absolute error for each component along the propagation time.
Before introducing the analysis, however, some initial remarks to clarify how this analysis applies to the PE game and on the underlying hypothesis are required. In the relative propagations, the spacecraft is modelled as a point mass, except in the Kechichian model due to the air drag computation. This analysis considers the propagation performance of a spacecraft, later referred to as the deputy, around another, the chief. To adapt this formulation to the PE game, where both objects manoeuvre to meet their objectives, both players are modelled as deputies of a common chief, represented by the undisturbed virtual motion of the evader on its operational orbit at the initial game time, successfully tracking the players' trajectories,
Recalling that the final aim is to develop an autonomous defensive system capable of handling AON measurements, a first crucial step of the analysis is to ensure the observability of all models. This is done through a generic symbolic analysis, verifying that all models are in principle observable, but without collocating them in any specific scenario, through Lie derivative.[1,20] Notably, all models but HCW retrieve an observability matrix N(x) of full rank, a sufficient condition to assert observability.[20] Concluding, as Yamanaka-Ankersen presents a state transition matrix formulation, its observability is assessed through a modified matrix process.[27] Additionally, the model's correct implementation is verified by comparison to propagations obtained by a verified numerical propagator[28] in MATLAB environment. Once the correctness and coherence of the framework of interest are established, a comprehensive sensitivity analysis is carried out to deeply understand and evaluate the various dynamic models' behaviour, performance, and robustness across different scenarios. The analysis focuses on the model's response to variations in the ECI operational orbit of the asset to protect, as well as to variations in the relative initial conditions of the attack. By investigating a wide range of orbital conditions, this approach aims to reveal any dependencies and bottlenecks of each model, and to ensure systematic propagation performance evaluations, a tailored-designed cost function is employed for each analysis.

Chief Orbit Variation The analysis varies the chief spacecraft, the one around which the relative motion occurs, and the orbital parameters. In particular, the semi-major axis a, the eccentricity e and inclination i are varied systematically in a triple nested iterative process in the range reported below:

$$\begin{aligned} \text{Semimajor axis: } a =&[6500,\ 46000]\ km\ -\ 100\,points \\ \text{Eccentricity: } e =&[0,\ 0.75]\ -\ 125\,points \\ \text{Inclination: } i =&[0,\ 90]\ -\ 90\,points \end{aligned}$$

This selection is such to encompass all near-Earth orbital regimes, from Geostationary Orbit (GEO) to Geostationary Transfer Orbit (GTO) and all Low Earth Orbits (LEO) regimes. The scope of the analysis may be expanded to generate a three-dimensional cube-like data structure based on the user preferences to suggest the best-performing dynamic model in each scenario, allowing for a dynamic modelling selection on board the spacecraft. Computationally, one could note that the generation of the eccentricity values is tuned to have a finer spacing for small values (¡0.1) for two reasons: first, most operational orbits and operational assets below to such eccentricity range, and second a greater sensitivity of the propagation performance is expected compared to large eccentricity values. For example, this strategy clarifies the maximum eccentricity values for which the near-circular hypothesis fails, or the lower bound for the application of the TH equations.
The propagation performance is evaluated through the cost function $J = \sum_{i=1}^{n} w_i \alpha_i$, where w_i represents the user-defined weights allocated to a given parameter α_i. In the analysis, the parameters of interest are thirteen: six RMSE, six maximum absolute error, one for each state component, and the computational time. Moreover, the quantities are scaled to allow for an even comparison among different units of measure.[1]

Deputy Orbit Variation The other factor that may vary across various PE engagements is the relative ignition condition of the attacking object in the LVLH frame, centred on a chief unperturbed spacecraft. The comprehensive and systematic analytical framework is organised as follows: four primary initial conditions are identified as most representative of key scenarios that may arise in various PE contexts, circular and eccentric LEO, GEO and a Highly Elliptical Orbit (HEO), whose orbital elements are reported in Table 1 with the propagation models whose hypothesis fit the scenario.

Table 1: Orbit configurations and propagation models used for the deputy sensitivity analysis

Label	Orbital Parameters	Dynamic Propagation Models
LEO	$a = 7000\,\text{km}$, $e = 5 \cdot 10^{-3}$, $i = 45°$	SOD, TOD, FNL, SCSW, TH, YAn, XW, KE
LEO2	$a = 14256\,\text{km}$, $e = 0.5$, $i = 82°$	TH, YAn, XW, KE
HEO	$a = 31628\,\text{km}$, $e = 0.7825$, $i = 63.4°$	TH, YAn, XW, KE
GEO	$a = 42164\,\text{km}$, $e = 5 \cdot 10^{-4}$, $i = 0.01°$	SOD, TOD, FNL, SCSW, YAn, TH, XW, KE

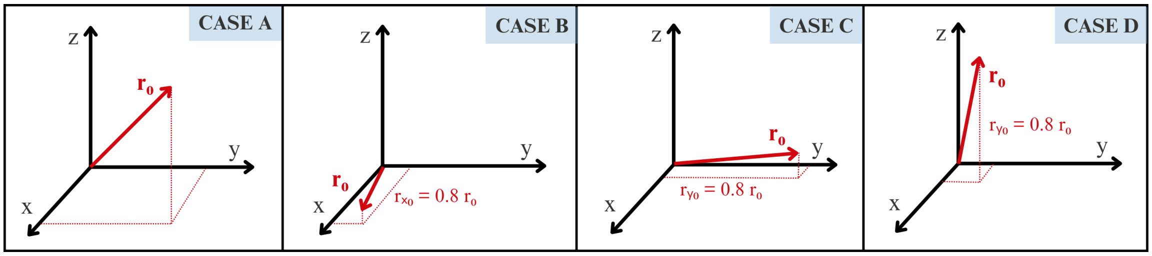

Figure 3: Initial relative condition on $\mathbf{r}$

The relative position and velocity are varied singularly. This means that the position vector is fixed, and the velocity components are varied, and vice versa, the velocity vector is fixed, but the position components are varied for each of these orbital scenarios.

In particular, the initial relative position is varied uniformly from 1m to 2km in an evenly spaced one-hundred-point vector, in four other different cases: evenly distributed in all directions, or strongly directional, as in Figure 3. The same process is carried out for the initial relative velocity, spanning from 1 m/s to 1 km/s in 100 intermediate values, again evenly distributed or strongly aligned. This allows to investigate whether some directions are consistently more intricate to predict or some geometry dependencies arise. The performance evaluation process is similar to the previous dimensionless one, but it neglects computational time, so that:[15]

$$J = \max_i \|W(\delta\mathbf{x}(t_i) - \delta\mathbf{x}_{\text{ref}}(t_i))\|_2 \quad \text{for } t_i \in [t_0, t_f]$$
$$W = \text{diag}(1, 1, 1, n_c^{-1}, n_c^{-1}, n_c^{-1}) \tag{4}$$

where $\delta\mathbf{x}(t_i)$ is the relative propagated state at time t_i and $\delta\mathbf{x}_{ref}$ represent the relative state from the propagator. W is a dedicated weight matrix that uniforms the units of measure to a length through the chief spacecraft mean motion $n_c = \sqrt{\frac{\mu}{a^3}}$.[15]

PE Game Implementation

The results of the sensitivity analyses on the initial inertial and relative conditions are exploited in the SDRE formulation to assess their behaviour in PE scenarios.

In this framework, SDRE control solutions are investigated coupled to those deemed the most performant models by the authors, but the flexibility of the cost function weights allows for diversified selections, based on the scenario at hand. Regardless of the dynamic model selected, through SDRE factorisation, the formulation is rearranged into a time-varying system in state space form, nonlinear in state and affine in control for each player. Then the game dynamics is expressed as the difference between the pursuer and the evader dynamics, so to write the differential system as:

$$\dot{\mathbf{x}}_{diff} = f(\mathbf{x_p}) - f(\mathbf{x_e}) + B_p\mathbf{u_p} + B_e\mathbf{u_e} \tag{5}$$

and through manipulations:

$$\dot{x}_{diff} = A(x)x_{diff} + B_p u_p + B_e u_e \tag{6}$$

where $x_{diff} = x_p - x_e$ $B_p = -B_e = B$ and $B = I_3$.
The control algorithm can be tailored to the PE game by considering both players' objectives in their cost function, as in Equation 7, as those are known reciprocally.

$$J_p = \frac{1}{2}\int_{t_0}^{\infty} \left(\mathbf{x}^\top(t)Q\mathbf{x}(t) + \mathbf{u}_p^\top(t)R\mathbf{u}_p(t) - \gamma^2\mathbf{u}_e^\top(t)R\mathbf{u}_e(t)\right) dt \tag{7}$$

J_p refers to the pursuer cost function, and due to the opposing objectives, $J_e = -J_p$. Additionally, in the PE game cost function in Equation 7, the parameter γ represents the *controllability ratio* of the players, defined as the ratio of the respective thrust-to-mass ratio as in.[8] To ensure the game completion, this parameter shall be set to a value greater than one, for the pursuer to outpower the evader. On the other hand, for gamma values lower than one, the evader is advantaged and the game may not be terminated, showcasing the escape. The saddle point equilibrium is obtained for the control actions u_p^* and u_e^*:

$$J_p(\mathbf{u}_p^*(\mathbf{x}), \mathbf{e}_p^*(\mathbf{x})) \leq J_p(\mathbf{u}_p(\mathbf{x}), \mathbf{u}_e^*(\mathbf{x})) \tag{8}$$

$$J_e(\mathbf{u}_p^*(\mathbf{x}), \mathbf{e}_p^*(\mathbf{x})) \leq J_e(\mathbf{u}_p(\mathbf{x}), \mathbf{u}_e^*(\mathbf{x})) \tag{9}$$

remarking on the one-sided advantage gained from the opponent's deviation from such a strategy.
The near-optimal control laws are expressed as:

$$\mathbf{u}_p^*(\mathbf{x}) = -\ R^{-1}B_p^T P(\mathbf{x})\mathbf{x} \tag{10}$$

$$\mathbf{u}_e^*(\mathbf{x}) = \ \gamma^{-2}R^{-1}B_e^T P(\mathbf{x})\mathbf{x} \tag{11}$$

$$\tag{12}$$

obtained by solving the ARE for P(x) at each time instance:

$$A^T(\mathbf{x})P(\mathbf{x}) + P(\mathbf{x})A(\mathbf{x}) + Q(\mathbf{x}) - P(\mathbf{x})(B_pR^{-1}B_p^T - \gamma^2B_eR^{-1}B_e^T)P(\mathbf{x}) = 0 \tag{13}$$

Notably, this formulation provides the control accelerations directly, so care shall be paid to tune the cost function parameters with the spacecraft mass to provide actionable thrust values. In particular, the study focuses on continuous low-thrust.

ANALYSIS AND DISCUSSION

In this section, the initial conditions and values of interest are clarified, showcasing the consequent results obtained, providing insights and discussions on the enhancement of evasive strategies in space.

Dynamic Models Analysis

The previously listed dynamic models are implemented in MATLAB, also exploited for the comparison among models, considering an absolute and relative tolerance of $1e^{-12}$.

Inertial Orbit Sensitivity Analysis The relative initial conditions considered along the analysis are highlighted in Table 2, and the reference quantities deployed for the spacecraft sizing in the Kechichian modelling are clarified in Table 3, picked such to provide a ballistic coefficient in a meaningful range for modern space applications.[29,30]

$x\ [m]$	$y\ [m]$	$z\ [m]$	$v_x\ [m/s]$	$v_y\ [m/s]$	$v_z\ [m/s]$
12	-60	5	-0.06	-0.02	-0.011

Table 2: Pursuer and Evader Relative Initial Conditions in LVLH

The weights considered in the cost function metric for the inertial orbit parameters for computational time and RMSE error, focusing on efficient and globally accurate propagations, and for the maximum absolute error are illustrated in Table 4.

Mass $[kg]$	Surface Area $[m^2]$	Drag Coefficient C_d
100	1	2.2

Table 3: Spacecraft physical parameters

Computational Time w_t	Max Error $w_{e_{max}}$	RMSE Error w_{RMSE}
0.45	0.1	0.45

Table 4: Weights considered in the Sensitivity Analysis Execution

The propagation time is set to three revolutions, thus based on the orbit size. An example of the output obtained is showcased in Figure 4. The figure shows the most performing model in the semi-major axis and eccentricity ranges in Section 2, for an inclination of $45°$. The blank zone corresponds to an unfeasible trajectory, whose pericentre is smaller than the Earth's orbital radius, with an additional 100 km safety margin.

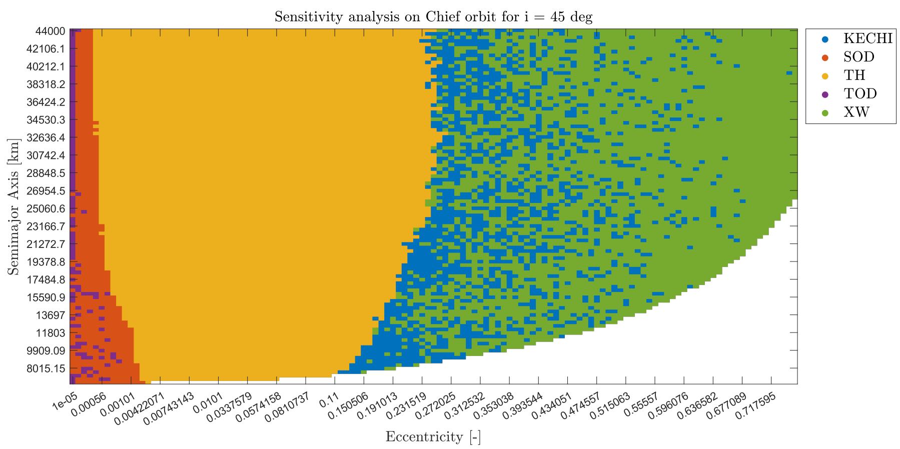

Figure 4: Sensitivity analysis results for chief virtual orbit variation for $45°$ inclination

The output segmentation in three major areas, based on the eccentricity and semi-major axis in this case, is fairly clear. The first region at the leftmost of the figure, where orbital eccentricities are low, and the simplest models manage to reach a comparable approximation to the more complex ones, but with a dramatic cut in computations, particularly as the inertial orbit, and so the period, enlarges. A second central region where simpler models fail, and the nonlinear ones are too demanding, favours the TH model in numerical form, and a last region where only the most complex and nonlinear models manage to provide an accurate estimation. This last region shows that the air drag can be neglected for such short periods, only gaining from computational reduction, as Kechichian and XW alternate, with the latter visibly more convenient for very high eccentricities. Notably, no TH closed-form solution arises. Upon close inspection, it is found that its propagation accuracy is the worst among all cases, although slightly counterbalanced by the lowest computational time.

Relative Orbit Sensitivity Analysis The procedure outlined in the previous section is executed, maintaining the fixed position and velocity vectors' components as in Table 5 and in Table 6. Figure 5 and Figure 6 showcase the results obtained for the circular LEO scenario, varying initial position and velocity vectors, respectively, in logarithmic scale. This scenario is reported as it allows for the consideration of most models, allowing a complete and thorough analysis. Here the SCSW implicit equation initial values could be tuned at each execution, allowing for its inclusion in the analysis.

r_x $[m]$	r_y $[m]$	r_z $[m]$
50	50	50

Table 5: Fixed initial relative position in the Chief's LVLH reference frame

v_x $[m/s]$	v_y $[m/s]$	v_z $[m/s]$
1	1	1

Table 6: Fixed initial relative velocity in the Chief's LVLH reference frame

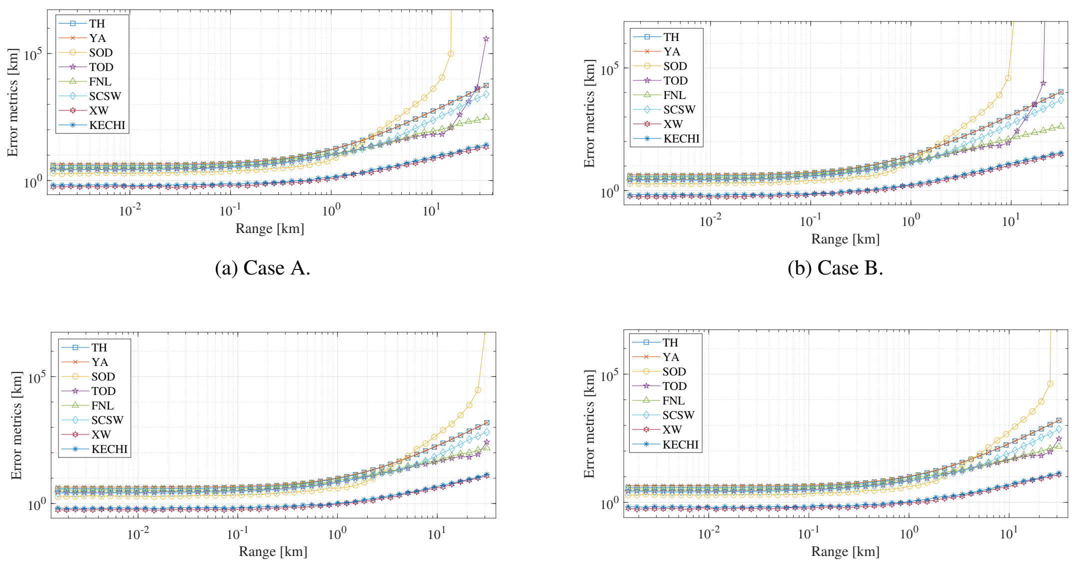

(a) Case A. (b) Case B. (c) Case C. (d) Case D.

Figure 5: Relative initial position variation, fixed relative initial velocity.

Here, the results are coherent with those of the previous analysis on the inertial orbit variations. The most complex non-linear models remain the most accurate across the entire span of values analysed, for any state component in any direction. Hence, XW and Kechichian models should be preferred if the computational power allows for the onboard exploitation, as the increased non-linearities would increase the system's observability with AON. Additionally, this analysis provides insights on the limits of applicability of the assumptions of each model. An example is provided by the HCW expansions to higher orders, as the propagation error significantly increases once the initial displacement is too high for the linearised dynamics hypothesis to hold, after a few hundred metres, and the same stance for the velocity, but amplified. Indeed, it is the full nonlinear expansion to provide the highest robustness performance, which is not linearised. Also the addition of J_2 provides enhanced robustness for the SCSW, behaving in comparably to the latter HCW expansion.

On the other hand, TH and YA provide increased robustness for the initial separations, holding propagation accuracy up to around one kilometre. Also, the robustness to higher relative velocity is showcased compared to the simpler solutions.

In general, aligning the initial position or velocity vectors to a given direction did not present major differences, highlighting how the shear separation magnitude affects the propagation rather than its disposition in space.

Regarding the other inertial orbits selected, provided the similarities found with the circular LEO case and the similarity of the solutions among the different directions, only the evenly distributed case is analysed for each case, allowing for a concise, yet exhaustive, overview. Figure 7 showcases the elliptical LEO analysis, excluding the HCW and expansions and derivatives, remarking on the enhanced accuracy provided by XW

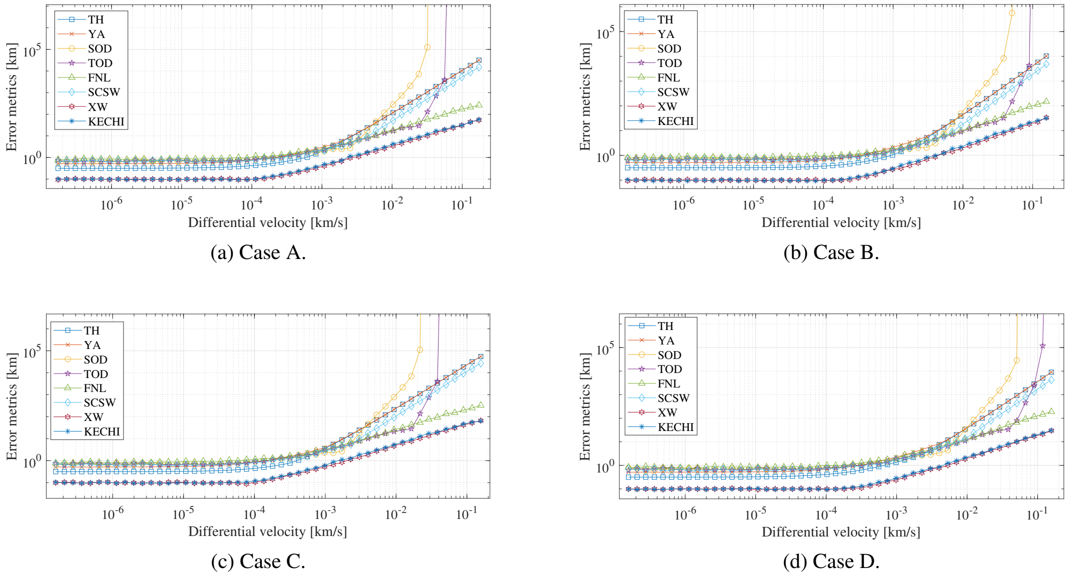

(a) Case A.

(b) Case B.

(c) Case C.

(d) Case D.

Figure 6: Relative initial velocity variation, fixed relative initial position

and Kechichian models, enhanced compared to the circular case, yet at the expense of a remarkable computational cost. The trend provided by TH and YA is similar to the circular case, but sharper for the error increase, losing accuracy faster. Figure 7 shows the propagation performance of the models for the HEO inertial case. Notably, the YA and TH models struggle to approximate the relative motion in any condition due to the high eccentricity, whereas XW and Kechichian allow for a satisfactory propagation in time, remarking on their robustness. However, the figure of merit trends provided are similar among the two models, both for position and velocity variations, with a progressive estimation error increase passed the hundred of metres separation for XW and Kechichian, whereas TH and YA remain stable for a longer span, although the initial error is remarkably higher. Concluding, Figure 9 reports the results of the sensitivity analysis for the GEO inertial orbit. Focusing on the position variation, it is immediate to see how the TH and YA performance overlap, resenting increased errors and remarking on the models' struggles in circular orbits. On the other hand, the HCW expansions provide different performance: the more complex third-order and full nonlinear expansions perform better than the simpler second-order and SCSW solutions, across the entire span. The latter models instead show performance among the worst in this analysis, comparable to YA and TH. They also present increased sensitivity to the initial range separation, with a steeper error increase curve. Last, the nonlinear Kechichian and XW present the best performance across the entire span of interest, joined by the highest robustness and stability. Focusing on the velocity variation, the figure of merit performance is the

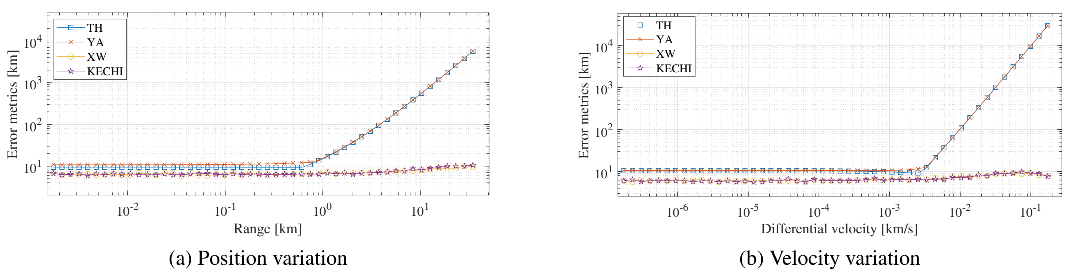

(a) Position variation

(b) Velocity variation

Figure 7: Relative initial position and velocity variation, for eccentric LEO orbit

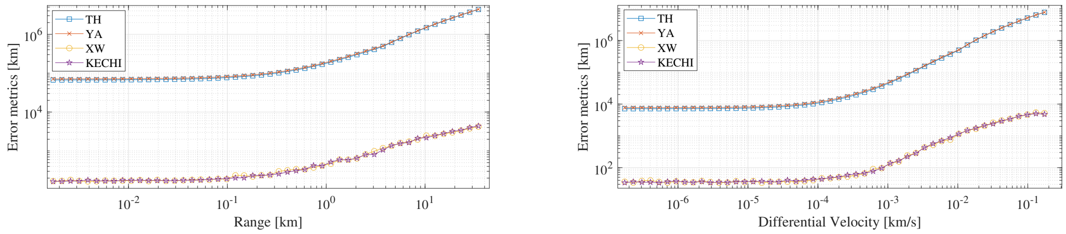

(a) Position variation

(b) Velocity variation

Figure 8: Relative initial position and velocity variation, for eccentric LEO orbit

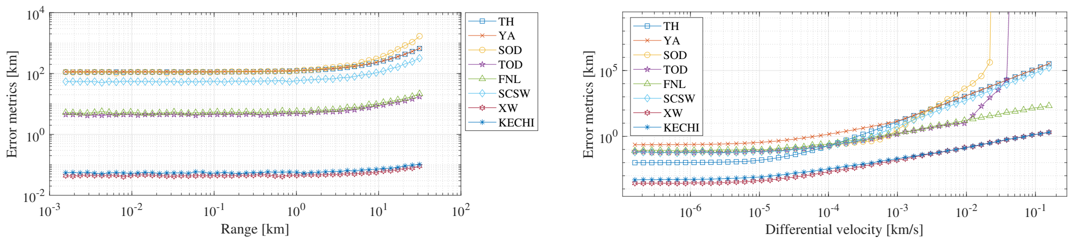

(a) Position variation

(b) Velocity variation

Figure 9: Relative initial position and velocity variation, for GEO orbit

poorest across all inertial scenarios analysed. All HCW models present significant divergence for relatively contained relative velocities, with only the full nonlinear expansion showing some robustness. Similarly, XW and Kechichian models show some increasing error trends, maintaining acceptable accuracies.
In conclusion, the sensitivity analyses conducted on the initial inertial and relative states are complementary, highlighting the different features and some common behaviours of the models. This analysis allows for a well-informed orbit modelling both in the upcoming part of the work and in operational scenarios through the cube-like data structure.

PE Game Resolution

The game is formulated into a MATLAB environment, exploiting *icare* to solve the ARE at each time step.[8] In the propagations, an absolute and relative tolerance of 10^{-12} is exploited, and the games are implemented in dimensional form to increase the computational efficiency using `ode113`. The game is considered terminated upon interception of the evader, thus when the game differential state maximum position component is lower than 10^{-8}. To match the current state of the PE games literature, and in the framework of a future filtering-based onboard estimation problem, the cost function weights are assumed constant along the game, and each matrix in the form: $R = r_i I_3$ $Q = q_i I_6$, with i = p, e. The game parameters considered in the simulations are reported in Table 7. The initial conditions of the PE game feature the initial relative state in Table 2 for the pursuer and the null vector for the evader, coincident with the centre of the virtual orbit's LVLH at initial time. The operative inertial orbit coincides with the elliptical and circular LEOs in Table 1, as those are deemed as more likely to be theatre of engagement scenario due to the assets services provided.

Q	R	γ^2
1	$1e^{-3}$	2

Table 7: ZSG Cost Function Parameters

Additionally, to verify the solutions obtained by the implementation investigated, those are verified against the solution obtained by Jagat-Sinclair (JS).[1,8] This PE game SDRE solution employs a two-body Keplerian-based dynamic model for linear and nonlinear formulations. The models selected for the implementation are XW and TH, according to the results of the previous analysis, but all models have been implemented for PE SDRE strategies, adapting to the user-demanded outputs of the sensitivity analysis. The resulting PE game's Game duration and computational time and are reported in Table 8 to provide a clearer representation and support for the discussion. The pursuer and evader are assumed to model the controls through the same dynamic modelling. The trajectories in the virtual orbit LVLH are highlighted in Figure 10 for the circular LEO case.

Model	Game Time $[min]$	Computational Time $[s]$
Circular LEO		
XW	102.5705	4.3530
TH	100.0533	3.0220
JS	97.6549	59.2516
KE	96.2539	68.8904
Eccentric LEO		
XW	101.1051	3.2403
TH	285.5425	2.9578
JS	97.6549	61.4147
KE	124.4125	29.0660

Table 8: Model performance in circular and eccentric LEO scenarios

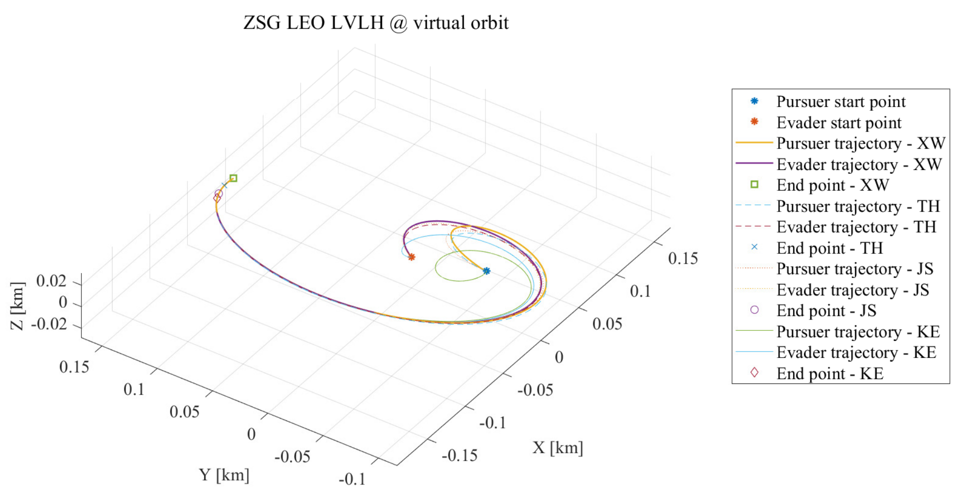

Figure 10: XW, TH, JS and KE models trajectories comparison, circular LEO in virtual orbit LVLH

One should note that Kechichian model has not been rendered dimensionless, due to more intricate process and multi-variables dependencies for each state element. Hence, its cost function weights have been multiplied according reference unit to match the problem with dimensions. In doing so, the R matrix has been multiplied by a factor 10^{-5} to provide controls and game times comparable to the other models, showcasing how each model, regardless of the adimensionalisation, reacts differently to the same objectives. This additional tuning, surely imperfect, justifies the shorter game time provided by the latter model, beyond the reference spacecraft sizes deployed, Table 3. On the other hand, the remarkably higher computational time is undisputed. Similarly, also the JS reference model shows a high computational burden. Differently, XW provides the longest game time, burdened by some computations when compared to TH, which instead provides a satisfactory game time. Overall ,the trajectories provided remain similar in the virtual orbit LVLH apart from Kechichian's solution, showing an initial higher deflection to then match the other PE games. To better understand the behaviour of the players along the game, the relative separation along each component in time is reported in Figure 11 for the circular virtual orbit scenario. Due to the SDRE formulation, one should note that those quantities are actually the driver of the game evolution, with the trajectories in the virtual orbit LVLH a mere consequence. Moreover, It can be seen that TH is the slowest to match the positions among all methods, showing different trend compared to the other models, particularly at the first game instances. On the other hand, Kechichian is similar to XW and JS, but it provides a strong initial deviation along the X component, visible also in the LVLH trajectories. Last, XW performs closest to the JS model, with minimum deviations across all components. In the eccentric scenario case instead, more evident differences arise in the virtual orbit LVLH trajectories in Figure 12, as well as in the relative dynamics evolution in Figure 13.In particular, the solutions of all the nonlinear models, although presenting increased differences in the eccentric case, the solutions remain in a constrained neighbourhood of space. Also the relative trajectories are comparable to the previous case, remarking on those model dependency from the initial conditions, yet showing robustness to such variations. On the other hand, TH being the only simple model provides a solution that is vastly different, particularly in terms of relative game. Despite the x component being similar to the other solutions, the y and z positions take a much longer time to match, with the latter showing a steep increase mid-game. This can be attributed to either the much lower modelling accuracy and precision provided by this simpler model, or by the significance of and sensitivity to the cost functions parameters.

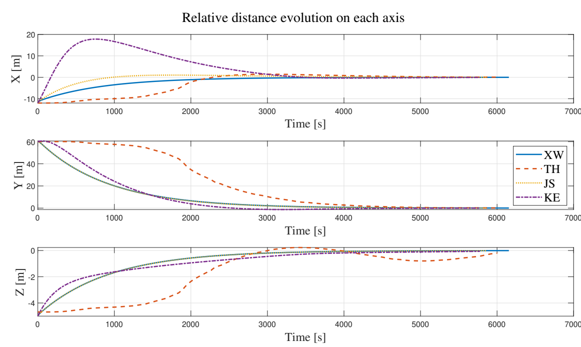

Figure 11: XW, TH and JS models trajectories comparison

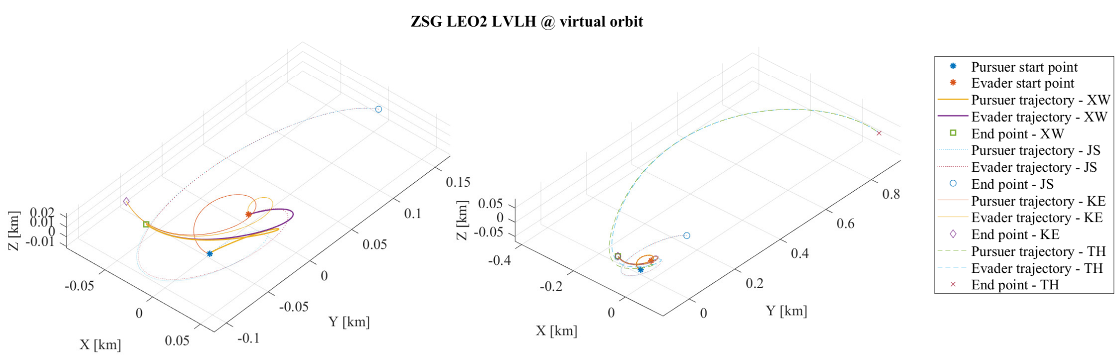

Figure 12: XW, TH, JS and KE models trajectories comparison, eccentric LEO in virtual orbit LVLH

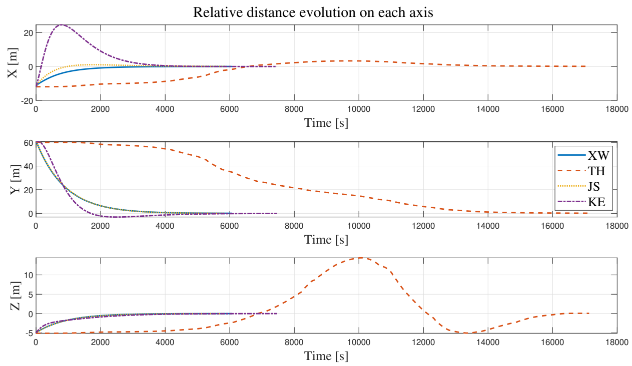

Figure 13: XW, TH, KE and JS trajectories comparison, virtual orbit LVLH

Sensitivity Analysis to the game parameters

As the in depth analysis of the game reference conditions has been concluded, the aim is now to characterise how the variations of the remaining game and cost functions parameters affect the dynamics of the former in terms of resulting controls and durations.
Hence, this first step focuses on varying the cost function values of the two players, whilst maintaining the same initial scenario as in Table 2 in the circular inertial orbit in Table 1. This is carried out systematically by defining a uniformly spaced grid of Q and R values, coincident for each player, as:

$$Q \in [10^{-5},\ 10^{5}],\ 500\ steps \tag{14}$$

$$R \in [10^{-5},\ 10^{5}],\ 500\ steps \tag{15}$$

evaluating a wide portfolio of objectives' setup and how each single parameter affects the game. The results of varying the cost function parameters are clarified in Figure 14 and Figure 15 for the JS and XW models, respectively. Upon close inspection, a first result to note is the verification of the consequences of Q and R variations, coincident to those mentioned in Section 2. Moreover, a property of the LQR can be extended to the SDRE case: the solutions to the PE game problem provide coincident durations and similar controls. This results stands for both measures, despite clearer for the JS results. This means that during the incomplete information games, the estimation process can be reduced in size by only estimating the ratio of Q and R, beyond the relative state.

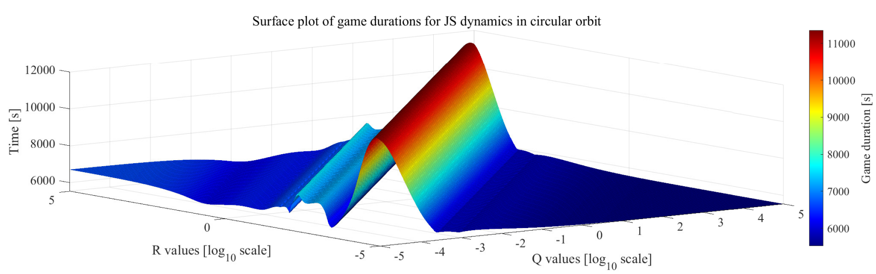

Figure 14: JS PE game durations varying Q and R

On the other hand, for each dynamic model, a pursuer-or evader-oriented regions are identified.
In general, the pursuer is at an advantage for higher Q values coupled with low R values, the scenarios where the control efforts are the highest. This is because the difference in controllability shows a stronger significance and effect on the dynamics the higher the control actions.
Focusing on the JS modelling first, the longest durations are identified in correspondence with the anti-diagonal direction, relating the extremes of each span of objectives: the lowest state matrix value with the

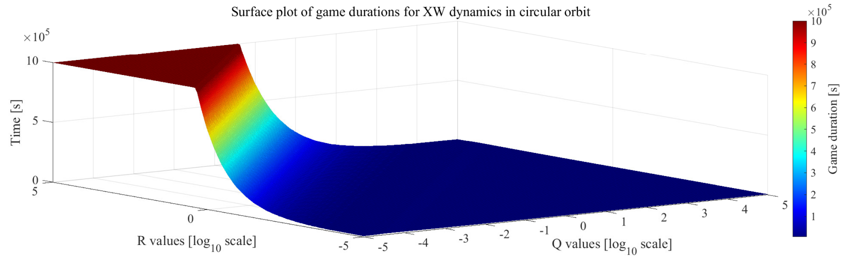

Figure 15: XW PE game durations varying Q and R

highest control penalties, and vice versa, leading to a constant ratio of Q and R equal to 1, whereas along the main diagonal direction, the game duration decreases as the distance from $\frac{Q}{R} = 1$ increases, showing the constant objectives ratio and game durations pattern. Additionally, as the control efforts decrease and R values increase, a second region of increased game durations arises, remarking the more favourable problem setup for the evader, providing longer survival.

When the controls and games are solved through the XW modelling, a different game time distribution is identified. In particular, this assumes a monotonically decreasing trend for the game duration as controls increase. It is evident that as the game objectives force a rather cautious pursuer approach to the engagement, through higher R and lower Q values, the evader presents better defensive chances. This is particularly true if the solution is compared to the simpler JS model one. Onthe other hand, for higher controls the solution provided is comparable to JS. Additionally, the game showcases a stronger sensitivity to the variation of the control penalties matrix R, when compared to Q and to the previous dynamic modelling.

Moreover, the game durations in this latter case are limited to one million seconds, limiting the remarkable computational burden and justifying the final plateau.

CONCLUSION

Overall, considering different dynamic modelling in the SDRE controls computation shows to have a broad effects on the PE game, even in the ideal scenario analysed where both players know each others state and cost function objectives exactly.

Different dynamic modelling lead to different trajectories in space, controls and durations, whilst ensuring computational efficiency and, fundamentally, state observability.

The consequences of different dynamic modelling are mainly highlighted in the variation of the cost function Q and R matrices, but also within the same scenario some differences have been shown to arise. It shall be considered that in this study only a preliminary and qualitative observability analysis was performed. Considering a quantitative measure of this property, either through insertion of some observability index in the dynamic modelling sensitivity cost functions or as a stand alone analysis, but in the same manner of the inertial orbit variation sensitivity investigation, would allow to have a pre-emptive estimation of the impact of the state and objectives estimation in the development of uncertain and imperfect PE games.

Along the work, the dynamic model that provides the best performance across all scenarios is XW, particularly if computational burden is accounted for. However, more simple models, like TH, can provide viable solutions for spacecraft with limited resources.

The study shows that perturbations have varying impacts on the system observability and modelling accuracy. For example the Earth's oblateness J_2 inclusion benefits both properties,[1,2] yet the Solar Radiation pressure has been shown to not enhance either one, especially if the computational burden is accounted for. The same argument in principle stands for other minor perturbations, such as lunisolar gravity, and is driven by the too short PE game duration for them to be effective. Thus case-dependant evaluations are recommended based on the required evasive pipeline operative scenario and requirements.

REFERENCES

[1] F. Mascellani and L. Oliva, "Autonomous evasive strategies for space defence: development and analysis of real-time on board interception-delaying algorithms," Master's thesis, Politecnico di Milano, 2024.

[2] G. Gaias and S. D'Amico, "Angles-only navigation and dynamics in satellite formation flying," *Journal of Guidance, Control, and Dynamics*, Vol. 37, No. 3, 2014, pp. 835–850.

[3] B. Gong, S. Wang, S. Li, and X. Li, "Review of space relative navigation based on angles-only measurements," *Astrodynamics*, Vol. 7, No. 2, 2023, pp. 131–152.

[4] R. Isaacs, "Differential games: Their scope, nature, and future," *Journal of Optimization Theory and Applications*, Vol. 3, 1969, pp. 283–295.

[5] T. D. Woodbury and J. E. Hurtado, "Adaptive play via estimation in uncertain nonzero-sum orbital pursuit evasion games," *AIAA Space and astronautics forum and exposition*, 2017, p. 5247.

[6] D. Shen, K. Pham, E. Blasch, H. Chen, and G. Chen, "Pursuit-evasion orbital game for satellite interception and collision avoidance," *Sensors and Systems for Space Applications IV*, Vol. 8044, SPIE, 2011, pp. 89–97.

[7] H.-X. Shen and L. Casalino, "Revisit of the three-dimensional orbital pursuit-evasion game," *Journal of Guidance, Control, and Dynamics*, Vol. 41, No. 8, 2018, pp. 1823–1831.

[8] A. Jagat and A. Sinclair, "Optimization Of Spacecraft Pursuit-Evasion Game Trajectories In The Euler-Hill Reference Frame," *AIAA/AAS Astrodynamics Specialist Conference 2014*, 08 2014, 10.2514/6.2014-4131.

[9] M. Capitanio, "Defense Tactics in Space: An Extensive Study on Spacecraft Evasive Strategies," Master's thesis, Politecnico di Milano, 2023/2024. Available online: Politecnico di Milano, Theses Repository.

[10] M. Pontani and B. A. Conway, "Numerical solution of the three-dimensional orbital pursuit-evasion game," *Journal of guidance, control, and dynamics*, Vol. 32, No. 2, 2009, pp. 474–487.

[11] D. Stupik *et al.*, "Differential Game Solutions for Orbital Maneuvering: A Case Study in Pursuit-Evasion," *Journal of Guidance, Control, and Dynamics*, Vol. 40, No. 1, 2017, pp. 123–135, 10.2514/1.G002000.

[12] K. Horie and B. A. Conway, "Genetic algorithm preprocessing for numerical solution of differential games problems," *Journal of guidance, control, and dynamics*, Vol. 27, No. 6, 2004, pp. 1075–1078.

[13] E. P. Blasch, K. Pham, and D. Shen, "Orbital satellite pursuit-evasion game-theoretical control," *2012 11th International Conference on Information Science, Signal Processing and their Applications (ISSPA)*, IEEE, 2012, pp. 1007–1012.

[14] H. D. Curtis, *Orbital mechanics for engineering students: Revised Reprint*. Butterworth-Heinemann, 2020.

[15] J. Sullivan, S. Grimberg, and S. D'Amico, "Comprehensive survey and assessment of spacecraft relative motion dynamics models," *Journal of Guidance, Control, and Dynamics*, Vol. 40, No. 8, 2017, pp. 1837–1859.

[16] K. Alfriend and H. Yan, "Evaluation and comparison of relative motion theories," *Journal of Guidance, Control, and Dynamics*, Vol. 28, No. 2, 2005, pp. 254–261.

[17] R. P. Russell, "Survey of spacecraft trajectory design in strongly perturbed environments," *Journal of Guidance, Control, and Dynamics*, Vol. 35, No. 3, 2012, pp. 705–720.

[18] D. P. Scharf, F. Y. Hadaegh, and S. R. Ploen, "A survey of spacecraft formation flying guidance and control. part ii: control," *Proceedings of the 2004 American control conference*, Vol. 4, Ieee, 2004, pp. 2976–2985.

[19] W. Clohessy and R. Wiltshire, "Terminal guidance system for satellite rendezvous," *Journal of the aerospace sciences*, Vol. 27, No. 9, 1960, pp. 653–658.

[20] E. A. Butcher, J. Wang, and T. A. Lovell, "On Kalman filtering and observability in nonlinear sequential relative orbit estimation," *Journal of Guidance, Control, and Dynamics*, Vol. 40, No. 9, 2017, pp. 2167–2182.

[21] S. A. Schweighart and R. J. Sedwick, "High-fidelity linearized J model for satellite formation flight," *Journal of Guidance, Control, and Dynamics*, Vol. 25, No. 6, 2002, pp. 1073–1080.

[22] Z. Dang, "Solutions of tschauner–hempel equations," *Journal of Guidance, Control, and Dynamics*, Vol. 40, No. 11, 2017, pp. 2956–2960.

[23] K. Yamanaka and F. Ankersen, "New state transition matrix for relative motion on an arbitrary elliptical orbit," *Journal of guidance, control, and dynamics*, Vol. 25, No. 1, 2002, pp. 60–66.

[24] J. A. Kechichian, "Motion in general elliptic orbit with respect to a dragging and precessing coordinate frame," *The Journal of the Astronautical Sciences*, Vol. 46, 1998, pp. 25–45.

[25] G. Xu and D. Wang, "Nonlinear dynamic equations of satellite relative motion around an oblate earth," *Journal of Guidance, Control, and Dynamics*, Vol. 31, No. 5, 2008, pp. 1521–1524.

[26] D. M. Kreps, "Nash equilibrium," *Game theory*, pp. 167–177, Springer, 1989.

[27] J. Sullivan, A. Koenig, and S. D'Amico, "Improved maneuver-free approach to angles-only navigation for space rendezvous," *26th AAS/AIAA space flight mechanics meeting, Napa, CA*, 2016.

[28] P. R. A. Gilz, "A non-linear simulator written in C for orbital spacecraft rendezvous applications.," *HAL*, 2016.

[29] M. Haneveer, "Orbital Lifetime Predictions: An assessment of model-based ballistic coefficient estimations and adjustment for temporal drag coefficient variations," 2017.

[30] G. Sebestyen, S. Fujikawa, N. Galassi, and A. Chuchra, *Orbits and Spacecraft-Related Geometry*. Springer International Publishing, 2018.